Impact of the 3d Electronic States of Cobalt and Manganese Phthalocyanines on the Electronic Structure at the Interface to Ag(111)

ARTICLE *in* THE JOURNAL OF PHYSICAL CHEMISTRY C · OCTOBER 2011

Impact Factor: 4.77 · DOI: 10.1021/Jp207568q

6 AUTHORS, INCLUDING:

Fotini Petraki

28 PUBLICATIONS **404** CITATIONS

SEE PROFILE

Heiko Peisert

University of Tuebingen

127 PUBLICATIONS **2,624** CITATIONS

SEE PROFILE

Umut Aygül

University of Tuebingen

14 PUBLICATIONS **168** CITATIONS

SEE PROFILE

Thomas Chassé

University of Tuebingen

230 PUBLICATIONS **2,566** CITATIONS

SEE PROFILE

THE JOURNAL OF PHYSICAL CHEMISTRY C

ARTICLE

pubs.acs.org/JPCC

Impact of the 3d Electronic States of Cobalt and Manganese Phthalocyanines on the Electronic Structure at the Interface to Ag(111)

F. Petraki,*[,†] H. Peisert,[†] F. Latteyer,[†] U. Aygül,[†] A. Vollmer,[‡] and T. Chassé[†]

[†]University of Tuebingen, IPTC, Auf der Morgenstelle 18, 72076 Tuebingen, Germany

[‡]Helmholtz Centre Berlin for Materials and Energy, Electron Storage Ring BESSY II, Albert-Einstein-Str. 15, 12489 Berlin, Germany

ABSTRACT: X-ray absorption (XAS) and photoemission (XPS) spectroscopy revealed a strong interaction at the interface between transition-metal Cobalt phthalocyanine (CoPc) and single-crystalline Ag(111) substrate. According the Co L-edge absorption spectra of ultrathin CoPc films, charge transfer between the metal 3d electrons and the underlying metallic substrate occurs. Less intense but comparable effects are also observed at the MnPc/Ag(111) interface for partially filled d levels of Mn. The nature of interacting orbitals is also discussed by means of resonant photoemission spectroscopy (ResPES) as well as in comparison with the CoPc/Au(100) interface studied previously.

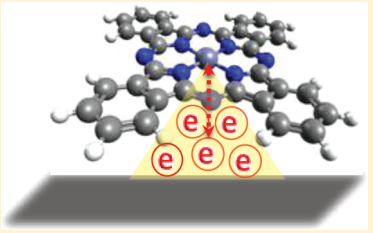

INTRODUCTION

Metal phthalocyanines have been the subject of much interest owing to their unique electronic and optical properties that can be technically exploited.[1−7] For example, it has been demonstrated recently that in particular transition-metal phthalocyanines (TMPcs) possess interesting magnetic properties due to the presence of the partially empty d levels of the central transition-metal atom,[8−12] and their application to spintronic devices is under investigation.[13−16] Therefore, detailed experimental studies of the interfaces between TMPcs and metallic substrates can give valuable insight into the understanding of the processes that take place at device interfaces. In particular, with respect to magnetic devices, the spin situation of the central metal atom of the TMPc may change distinctly at the interfaces. Because TMPcs are small molecules that can be easily evaporated under controlled vacuum conditions, they are well-suited as representative model systems for the investigation of the fundamental properties (electronic, optical, and magnetic) of many other transition-metal-containing materials. In the present work, we focus on interfaces between Ag(111) and CoPc or MnPc. The investigated TMPc's (TM: Co, Mn) are planar molecules with D_{4h} symmetry; the central metal atom is surrounded by the *Pc* ring (Figure 3, inset). Despite a large number of experimental and theoretical studies in the past decades, driven by the excellent perspective for various applications, essential details of the electronic structure and excitations of CoPc and MnPc are still unclear,[13,17−22] in particular, the role of the TMPc metal atom in the interface formation. Our studies have been carried out by photoexcited electron spectroscopies such as X-ray photoemission (XPS), X-ray absorption (XAS, NEXAFS), and resonant photoemission spectroscopy (ResPES) with the intention to understand the interference of the 3d states of the central transition-metal atom in the absorption configuration as well as the electronic properties of the interface. XAS provides information about the nature of the empty molecular orbitals of the absorbing atom. It monitors transitions from core level to unoccupied states (to the lowest unoccupied molecular orbitals, LUMO). Because of the resonant nature of the electron emission process near the XAS edge, with ResPES, it is possible to shed light on the nature of the spectral features in the valence band. Therefore, this technique is suitable to identify spectral features in the valence band and correlate them with specific chemical sites inside the molecule and to unoccupied states.[23] ResPES has been successfully applied also in the case of metal phthalocyanines.[23,24]

EXPERIMENTAL METHODS

The XAS and the resonant photoemission measurements were carried out at the third generation synchrotron radiation source BESSY II (Berlin) using the Optics-beamline and the end-station SurICat. The photon energies were calibrated comparing the binding energy (BE) of Au $4f_{7/2}$ peak excited by first- and second-order light. XAS were acquired in total-electron yield (TEY) mode, measuring the drain current, with a resolution of ∼100 meV at a photon energy of 400 eV. Detailed description for the experimental process can be found elsewhere.[25] The Ag(111) substrate was cleaned prior to organic film deposition by repeated sputtering-annealing treatment, and the cleanliness was checked by XPS. Ultrathin films of CoPc and MnPc, purchased from Aldrich, were thermally evaporated on the substrate in ultrahigh vacuum (base pressure $<1 \times 10^{-8}$ mbar) from a temperature-controlled evaporation cell. The deposition rate, monitored by a quartz crystal oscillator, was about 1 to 2 Å/min. The thickness of the TMPc films ranged from monolayer to ∼30 Å. The comparison of the film thickness determined using the quartz microbalance

Received: August 7, 2011
Revised: September 15, 2011
Published: September 18, 2011

with the attenuation of the intensity of the Ag 3d substrate peak in photoemission suggested an almost a layer-by-layer growth in each step of deposition.

RESULTS AND DISCUSSION

Chemical interactions at interfaces may result in new spectral features in XAS spectra. Because XAS spectral features are in addition strongly polarization-dependent,[18,25] the molecular orientation has to be known for each step of deposition. Therefore, we consider first the orientation of the TMPc's on a well-defined metallic surface. In XAS, the absorption process is controlled by selection rules, and the polarization of the synchrotron radiation can therefore be utilized to probe the symmetry character of the different molecular orbitals of well-oriented systems.[26,27] Because the intensities of the spectral features depend on the orientation of the molecular symmetry planes relative to the electric field vector E of the incident radiation light, XAS permits the determination of the orientation of adsorbed molecules with respect to the surface plane.

By analogy to related systems, it can be expected that the aromatic CoPc molecules adsorb on the atomically flat metal surface in a flat-lying geometry with maximum interaction of the extended π system and d orbitals of the transition metal with the substrate.[28] In some cases, however, specifically for rough substrates, a change of the molecular orientation as a function of the film thickness was observed.[28,29] To rule out such a behavior in the present experiments, we discuss in the following the orientation of the thickest films. Because a common carbon contamination of beamline components often hinders the detailed analysis of carbon edges, in particular, for monolayer systems, for the determination of the molecular orientation of metal phthalocyanines the analysis of N 1s-π^* excitations is favorable.[28]

In Figure 1, series of Nitrogen K XAS spectra for ~3 nm thick CoPc (Figure 1a) and MnPc (Figure 1b) films deposited on Ag(111) are displayed at different incidence angles of the incoming p-polarized light (inset of Figure 1a) with respect to the substrate surface. In both cases, four sharp core excitation lines labeled as A−D are observed at grazing incidence (θ = 10°). Similarly to other phthalocyanines, features in this energy range can be mainly attributed to transitions of N 1s electrons into unoccupied π^* states, polarized perpendicular to the molecular plane.[9,28,30] The broad features at higher photon energies (E, F) are due to transitions from N 1s orbitals into σ^* states. For both CoPc and MnPc, a very clear angular dependence of the π^* resonance intensities (E = 400−405 eV) with a maximum intensity at grazing incidence (θ = 10°) is observed. The σ^* resonances exhibit the opposite polarization dependence. This indicates the presence of lying molecules at this coverage; that is, a change of the orientation from "lying" to "standing" with increasing film thickness, as discussed above, can be ruled out at these film thicknesses. However, from Figure 1, it is clearly visible that at normal incidence (θ = 90°) some intensity in the energy range of π^* resonances remains. The presence of a weak, in-plane polarized transition in the same energy range as the π^* resonances was also found for NiPc[31] and CuPc.[32] In the case of CuPc, the remaining intensity was associated either with a rehybridization of the LUMO states localized on some N atoms or with a distortion of some bonds of N atoms in the CuPc atomic backbone.[32] The in-plane polarized spectral features at normal incidence (θ = 90°) in the range of π^* resonances are clearly more pronounced for CoPc and MnPc (Figure 1). We suggest a significant

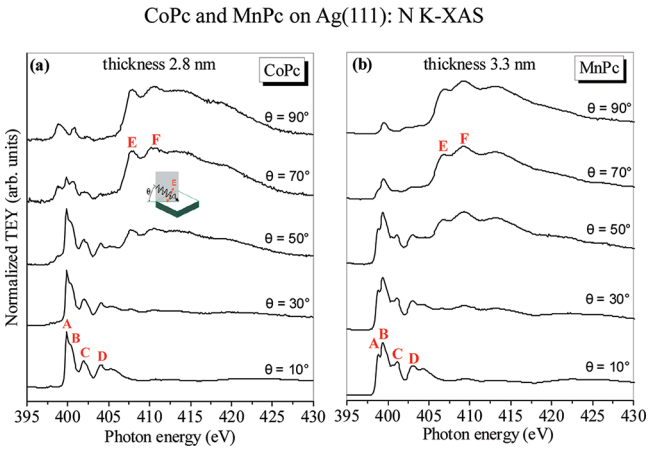

Figure 1. N K XAS absorption spectra for a (a) 2.8 nm CoPc and (b) 3.3 nm MnPc film evaporated on Ag(111). The spectra were recorded with different angles of beam incidence. (θ = 90° corresponds to normal and θ = 10° corresponds to grazing incidence; see inset of panel a.)

contribution to these features due to the mixing of N p-states with states of the central metal atom, that is, by a hybridization of unoccupied nitrogen-related states with d orbitals of the central metal, although second-order excitations of L2 may also contribute in the π^* region especially in the case of CoPc. As the energy of metal related states depends clearly on the central metal atom of the phthalocyanine molecule,[6,33] it can be expected that also the strength of such hybridization depends on the metal atom. In general, this might result in hybrid orbitals with different character, as recently reported for MnPc.[15] In particular, for CoPc, we recognize that the residual features in the π^* region at θ = 90° are not at the same energetic position as the most prominent π^* transition (feature A) at θ = 10°, verifying their different origin. Therefore, despite this appearance of states of different electronic origin at the same energy, the conclusion regarding lying molecules holds.

In the case of CoPc on gold, we detected recently significant changes of Co-XAS spectra at the interface, most likely due to charge transfer processes involving mainly the Co atom.[18,25] Because the interaction to silver is expected to be similar or even stronger, a comparable behavior might confirm this assumption. To acquire additional information about this interaction, we performed complementary XAS measurements at the Co L-edge for CoPc on Ag(111). In Figure 2, the corresponding Co $L_{2,3}$ XAS spectra are presented for nominal CoPc coverage of 2.8 (Figure 2a,b), 1 (Figure 2c), and 0.5 nm (Figure 2d). The features in the photon energy region between 775 and 785 eV are due to transitions from the Co $2p_{3/2}$ orbitals into unoccupied d orbitals (L_3 spectra), whereas the broad feature in the range of 792−797 eV is attributed to transitions from the Co $2p_{1/2}$ levels (L_2 spectra). The general features of the spectra in Figure 2a for the 2.8 nm thick film are in good agreement with the corresponding spectra for CoPc on Au(100).[25,32,35] In the following, we will focus on the Co $2p_{3/2}$ related transitions; a zoom into this region for different film thicknesses is displayed in Figures 2b−d. Because of the known absorption geometry of the molecules, angle-dependent XAS maps transition into different empty molecular orbitals and thus give information about the unoccupied electronic structure. According to Figure 2b, the spectrum at grazing incidence (θ = 10°) for a 2.8 nm CoPc film is mainly composed of feature A at the lowest energies (778.2 eV). The intensity of A gradually attenuates by changing the polarization angle. At normal

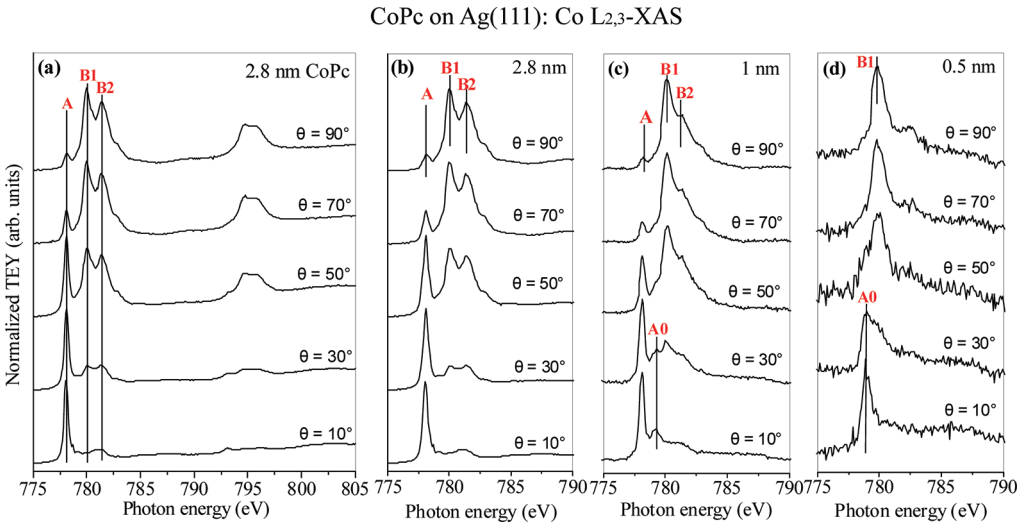

Figure 2. Co $L_{2,3}$ edge XAS spectra for the CoPc/Ag(111) system at an organic film thickness of (a,b) 2.8 nm, (c) 1 nm, and (d) 0.5 nm recorded at different angles of photon incidence.

incidence, the spectrum is dominated by the B1 (780.0 eV) and B2 (781.4 eV) features. As the molecules adsorb in a lying geometry on Ag(111), the A transition is vertically polarized to the molecular plane (*z*-polarized), whereas B1 and B2 are *xy*-polarized transitions (within the molecular plane), nearly identical to the Au substrate at similar coverage. (See refs 25 and 34.) In the case of thinner films with ~1 nm CoPc coverage (~3 ML) at grazing incidence (Figure 2c), another feature called A0 appears in the spectra, which was not present in the spectra of the thicker film. A0 vanishes at normal incidence of the synchrotron light quite similar to A.

For the 0.5 nm coverage (Figure 2d), the Co excitation spectrum at grazing incidence is dominated by the (new) A0 feature, whereas peak A, which dominates the spectra at higher film thickness, has completely disappeared. As already indicated in the spectra of the 1 nm thick film, A0 seems to have the same angular dependence pointing to a similar orbital symmetry as feature A. At normal incidence ($\theta = 90°$), A0 has completely disappeared and feature B1 dominates the spectrum (Figure 2d), whereas the relative intensity of B2 is much weaker than for the thicker films (Figure 2b,c). This may indicate a partial filling of the related *xy*-polarized states, for example, through charge transfer at the interface or redistribution of the d electrons at the Co atom. However, multiplet effects determine significantly the shape of both XAS and XPS spectra due to the strong overlap of the core wave function with the valence wave functions. For Co 2p, the final state of the XAS process consists of a partially filled $2p^{-1}$ core hole state and incompletely filled 3D valence states, leading to several final states terms that affect the shape of the XAS spectrum. Moreover, at interfaces, several parameters may change, such as the crystal field splitting or the on-site Coulomb interaction, affecting also the spectra shape.

In Figure 3, the related Co $2p_{3/2}$ XPS spectra are presented for different CoPc coverages on Ag(111). A significant change is observed in the peak shape by increasing the organic film thickness. The spectrum at ~0.5 nm (1 to 2 ML) is dominated by an intense and quite sharp peak appeared at the low BE side, whereas the overlayer spectrum is composed of a rather broad structure at higher BE. No significant changes were observed in the case of the nitrogen and carbon core level spectra of CoPc on Ag(111), indicating a particular interaction at the Co site of the molecule.

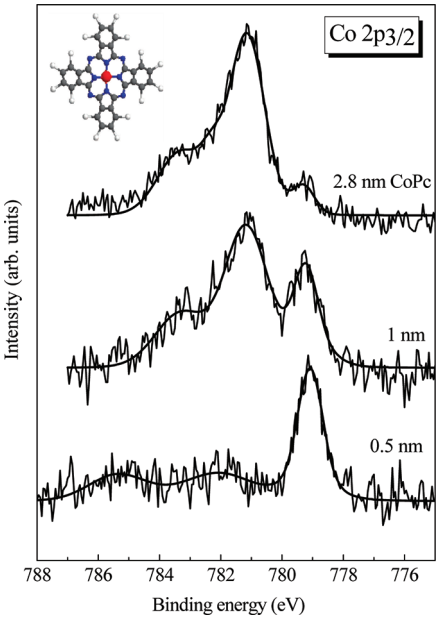

Figure 3. X-ray photoelectron spectroscopy (XPS) spectra of Co $2p_{3/2}$ core levels for CoPc on Ag(111).

The results remind now to the recently investigated CoPc/Au(100) interface; in particular, the related Co $2p_{3/2}$ XPS spectra are in good agreement,[25] pointing to a change of the electronic configuration of the Co atoms in both cases. Similar spectral shape was recently observed at the F_{16}CoPc/Ag(111) interface.[36] Such electronic interactions at interfaces may now result in new electronic states in the band gap of the organic semiconductor, as revealed by ultraviolet photoelectron spectroscopy (UPS) for metal phthalocyanines on metallic substrates (see, e.g., refs 18 and 37). In particular, for the CoPc/Au interface, such gap states were discussed in detail in ref 18.

Comparing the Co $L_{2,3}$ XAS for CoPc/Ag(111) (Figure 2) and CoPc/Au(100),[25] the behavior of feature B2 is very similar for both systems: B2 disappears in the ultrathin films of 1 to 2 monolayers, indicating clearly an interfacial charge transfer at

both interfaces. The presence of a feature like A0 is not detectable at the CoPc/Au(100) interface.[25] This can be seen more clearly from a direct comparison of the corresponding Co L-edge absorption spectra on gold and silver substrates displayed in Figure 4 for a CoPc coverage of 1 nm. A possible explanation of this phenomenon could be that the interaction between wave functions of Co and the metal substrate results in a pair of new levels whose energies are different for Au(100) and Ag(111). In this picture, the feature A0 could be due to transitions into the new (unoccupied) electronic level. If the energetic position of A0 at the interface to Au(100) is closer to A, then this feature may not be resolved in the spectra. In other words, the charge transfer between the metal d states and the substrate (Au and Ag) may lead to slightly different electronic situations at both interfaces. In general, the explanation of the above phenomena in terms of charge transfer processes agrees well with the most of the recent studies presented in the literature for related systems.[11,38−43] For example, STM studies on the CoPc/Au(111) and CoPc/Ag(111) interfaces[11,39] revealed an interaction between the organic layer and the substrate due to one unpaired d-electron of the Co atom.

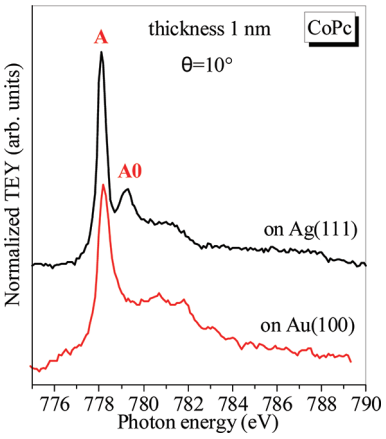

Figure 4. Comparison between Co $L_{2,3}$ XAS absorption spectra for 1 nm CoPc on Au(100) and Ag(111) recorded at 10° of photon incidence.

The question arises now whether such kind of strong interaction also occurs in the case of other TMPcs with partially filled d levels. To investigate the impact of the transition-metal 3d levels of the MPc's central metal ion in the absorption configuration and the electronic structure, XPS and XAS studies at the MnPc/Ag(111) interface were performed. In the case of Mn 2p XPS spectra (not shown), however, the counting statistics caused by low photoemission cross sections and the fact that a monolayer coverage of MnPc corresponds to a ∼1/40 monolayer Mn makes it difficult to distinguish different spectral features exactly. We focus therefore on XAS measurements. Figure 5 presents three series of Mn $L_{2,3}$ XAS spectra for 3.3, 1.3, and 0.7 nm (= 2 ML) thick MnPc films evaporated on Ag(111) taken at different photon incidence angles. Analogously to the Co excitation spectra in Figure 2, two groups of Mn 2p excitations with different polarization dependence are visible for the MnPc/Ag(111) in "bulk-like" thin film of ∼3 nm (Figure 5a). The L_2 (650−658 eV) and L_3 (640−648 eV) absorption peaks are due to $2p_{1/2} \rightarrow 3d$ and $2p_{3/2} \rightarrow 3d$ electron transitions, respectively. The L_2 and L_3 peak separation corresponds well to the $2p_{1/2}$ and $2p_{3/2}$ spin−orbit splitting for Mn,[44,45] which is 11.2 eV. At grazing incidence (θ = 10°), two peaks labeled as A1 (640.1 eV) and A2 (641.4 eV) dominate the L_3 spectra for both 1.3 (Figure 5c) and 3.3 nm (Figure 5b) of thickness, whereas at normal incidence (θ = 90°) three features (B1, B2, B3) at 639.4, 640.8, and 642.4 eV can be clearly distinguished within the L_3 peak. Similar to the CoPc/Ag(111) interface, features A1 and A2 observed at grazing incidence are attributed to *z*-polarized, whereas B1, B2, and B3 are *xy*-polarized features. Thickness-dependent differences in the spectra are essentially related to the intensity ratio of B features. Most visibly, the relative intensity of B2 is decreased at lower coverages, which points to a (partial) filling of the related orbital. The "partial" filling might be related to the fact that we average over about two monolayers, whereas the charge transfer occurs only directly at the interface. Although MnPc is an open shell molecule similar to CoPc with the metal d levels partially filled, only small changes are observed in the Mn-XAS spectral series going from the overlayer to the thin films. This difference compared with the corresponding CoPc-related absorption spectra may point to a weaker change of the whole electronic configuration at the metal atom of the *Pc* accompanied by the charge transfer process at the interface to Ag(111). Therefore, we may

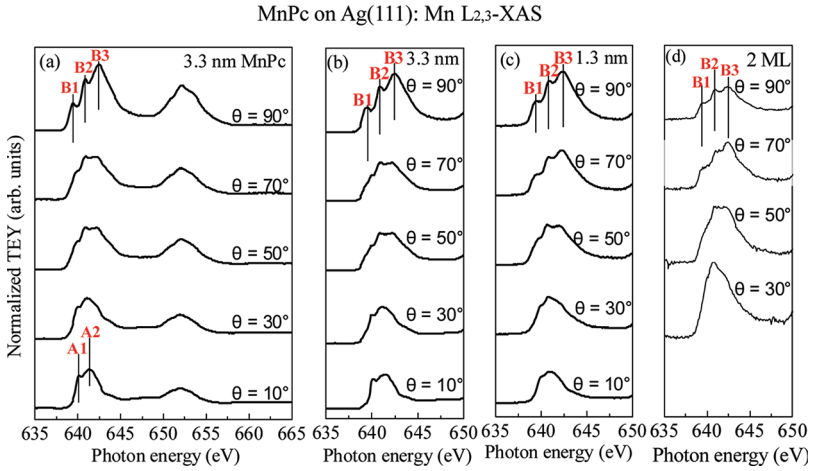

Figure 5. Mn $L_{2,3}$ edge XAS spectra for (a,b) 3.3 nm, (c) 1.3 nm, and (d) 0.7 nm (2 ML) MnPc coverage on Ag (111). The spectra were recorded at different angles of beam incidence with respect to the surface.

dx.doi.org/10.1021/jp207568q |*J. Phys. Chem. C* 2011, 115, 21334–21340

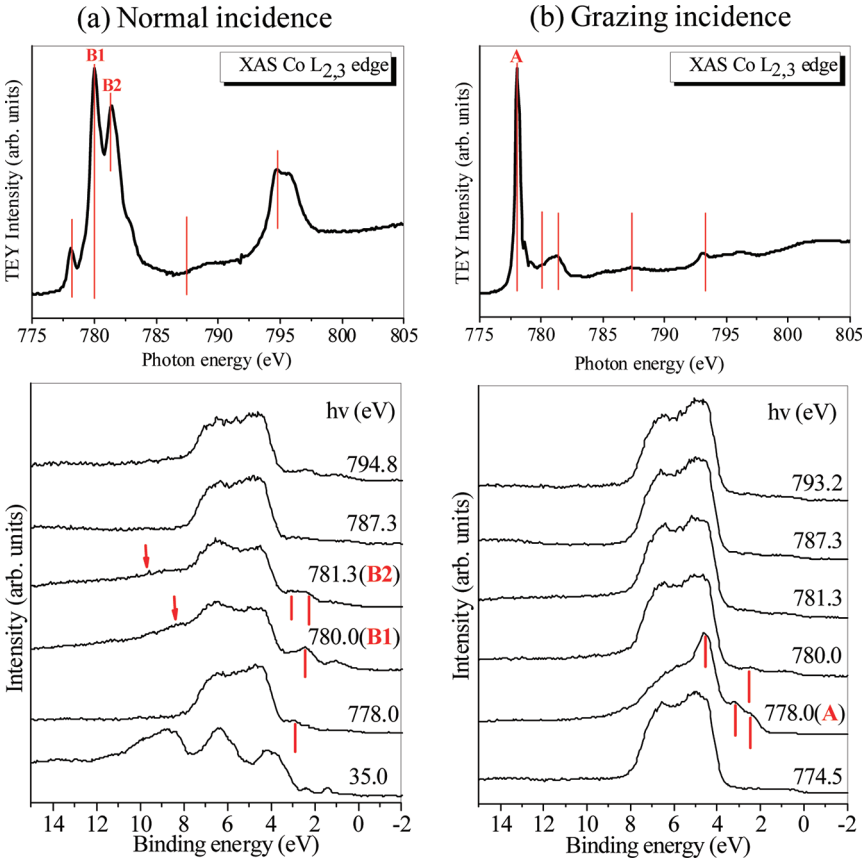

Figure 6. Resonant photoemission spectra acquired at normal (a) and grazing (b) incidence for a thick (2.8 nm) CoPc film deposited on Ag(111). In the upper panel, the corresponding Co $L_{2,3}$ edge XAS spectrum is shown for normal and grazing incidence of polarized light.

conclude that interface properties are significantly related to the energetic position of the metal states under consideration and their occupancy. To compare the electronic situation for CoPc and MnPc in more detail, we will discuss the electronic configuration of the central metal atom qualitatively. From crystal field splitting theory, we expect for TMPc's with flat geometry (D_{4h}) that the 3d orbitals transform as a_{1g} (d_{z^2}), b_{1g} ($d_{x^2-y^2}$), e_g (d_π or $d_{yx,zy}$), and b_{2g} (d_{xy}).[46] Even at monolayer coverage where C_{4v} symmetry can be expected, that is, due to a bending of the molecule or due to the formation of chemical bonds, the splitting of the energetic states will be the same as in the case of D_{4h} symmetry. However, the exact electronic configuration is determined to a large extent by further parameters; Coulomb and exchange interactions between the d electrons as well as spin−orbit coupling has to be taken into account.[12,47] For CoPc, most theoretical studies agree that the highest energetic state b_{1g} ($d_{x^2-y^2}$) is completely empty, however, different results were obtained for the remaining single occupied or d_{z^2} or $d_{yx,\ zy}$ states.[12,33,46,48] Similar for MnPc, different results are currently discussed in the literature, for example, one discussed electron configuration is d_π (e_g ($\downarrow$)), d_{xy} (b_{2g} ($\downarrow$)), d_{z^2} (a_{1g} ($\downarrow$)), $d_{x^2-y^2}$ (b_{1g} ($\uparrow$)), and $d_{x^2-y^2}$ (b_{1g} ($\downarrow$)).[49] Therefore, the different theoretical results make the discussion complicated. If we try nevertheless to relate the above d states with the features observed at the XAS spectra, in the case of the Co $L_{2,3}$ spectrum (1 nm of coverage), from their polarization dependence, the very intense feature (A) at ~778 eV as well as the less intense feature (A0) at ~779 eV can be assigned to states in *z*-direction (a_{1g}), whereas the features B1 and B2 are related to the initially completely empty b_{1g} energetic state. In the case of the 0.5 nm thin film, the disappearance of feature B2 indicates that the corresponding electronic states become filled by electrons donated from the substrate, whereas the domination of the $\theta = 10°$ spectra from A0 depicts the involvement of the a_{1g} d electrons in the transition process.[38] As previously mentioned, A0 may arise from a hybridization with the substrate, with a major influence of the d states delocalized out of the molecular plane. At the MnPc/Ag(111) interface, however, because the Mn-related unfilled levels are closely in energetic position,[50] the situation becomes more complicated. In this case, the Mn-XAS features are broader compared with the corresponding Co-XAS; therefore, an additional A0 feature could be also hidden. The decrease in the relative intensity of B2 at a coverage of about one to two monolayers indicates, however, that the same levels are involved in the likely charge-transfer process. However, as discussed above, for a more exact description of the electronic situation at interfaces, several parameters may change, resulting in a redistribution of the electrons (i.e., crystal field splitting, Coulomb, and exchange interaction). In addition, multiplet effects, which determine the spectral shape to a large extent, are not considered in this discussion.

To shed light on the electronic nature of the spectral feature B2, which is obviously mainly involved in the charge transfer processes at the interface to Ag(111), resonant photoemission measurements were performed on the CoPc/Ag(111) interface. ResPES was carried out by sweeping the photon energy in discrete steps over the respective absorption Co $L_{2,3}$ edge while

detecting electrons emitted from the valence region. In general, the spectra shown in Figure 6 for a 2.8 nm CoPc film deposited on Ag(111) agree well with recently published results for CoPc on Au(100).[34] However, because at these excitation energies valence band spectra of ~3 nm thick *Pc* films on Au or Ag are determined by substrate-related features, and the access to CoPc features at binding energies between 2 and 4 eV is hindered in the case of Au, due to an overlap with the Au-d band emissions. Because the XAS spectra (Figure 2) are polarization-dependent, also the ResPES data in Figure 6 depend on the polarization of the incident light; that is, a strong resonant enhancement of spectral features can be observed only if the excitation into an empty state is possible. In particular, at normal incidence of light (Figure 6a), an excitation into the *xy*-polarized B1 and B2 transitions between 780 and 782 eV is possible in XAS, resulting in a significant enhancement of spectral features near the HOMO (binding energies of 1−3 eV). Thereby, the enhancement of lowest-lying feature is strongest at the excitation energy of the B1, pointing to a significant contribution of the involved orbital to the HOMO. The development of the above-mentioned resonant spectral features is accompanied by a clear background increase within the resonance, pointing to a more delocalized Co-related states on the site of the excitation (more in the *xy*-direction compared with the *z* direction). (See ref 34.) In contrast, at grazing incidence (Figure 6b), it was found that *z*-polarized transitions at ~778 eV (feature A in the upper XAS spectrum) related to the molecular axis cause an enhancement of a valence band feature at ~4 eV. Additionally, the development of resonant features between 2 and 3 eV for excitation energy of 778.0 eV occurs, which was hidden by substrate features at CoPc/Au(100).[34] Although the enhancement of the same features is more pronounced at normal incidence of light (mainly at *xy* direction), this may imply that the excitation of an electron into a particular unoccupied orbital causes not necessarily a resonant emission from the same orbital. The absence of a clear background increase within the resonance points to localized Co-related states in the *z*-direction (so-called "participator transitions"; for a detailed discussion, see ref 34).

In general, the presence of resonant enhancements of valence band features in ResPES for the excitation energies corresponding to the absorption Co $L_{2,3}$ edge illustrate that these resonant features have their origin in Co 3d-derived orbitals; that is, Co (3d) orbitals contribute considerably to the valence level structure of the CoPc molecule. The enhanced resonant features at the B1 position are close to the HOMO, at 2 to 3 eV BE.

SUMMARY

Synchrotron-based photoexcited electron spectroscopic measurements revealed the presence of charge transfer between transition- metal phthalocyanines (CoPc, MnPc) and Ag(111) substrate. A significant charge donation from the underlying metallic substrate to the central metal Co atom of the phthalocyanine molecule leads to a redistribution of the 3d electrons inducing changes in the Co-related absorption spectra. Although in the case of the MnPc changes in XAS spectra are less pronounced, charge transfer processes are likely at the interface to Ag(111).

AUTHOR INFORMATION

Corresponding Author

*E-mail: fotini.petraki@uni-tuebingen.de. Tel: ++49 7071 29 76252.

ACKNOWLEDGMENT

The work was supported by the German Research Council Ch 132/20-2. We acknowledge the Helmholtz-Zentrum Berlin - Electron storage ring BESSY II for provision of synchrotron radiation at the Optics-beamline. Financial travel support by BESSY is gratefully acknowledged. We thank W. Neu for technical support.

REFERENCES

(1) Dini, D.; Hanack, M. *J. Porphyrins Phthalocyanines* **2004**, *8*, 915–933.
(2) Gao, Y. *Mater. Sci. Eng., R* **2010**, *68*, 39–87.
(3) Gould, R. D. *Coord. Chem. Rev.* **1996**, *156*, 237–247.
(4) Peisert, H.; Knupfer, M.; Schwieger, T.; Auerhammer, J. M.; Golden, M. S.; Fink, J. *J. Appl. Phys.* **2002**, *91*, 4872–4878.
(5) (a) Petraki, F.; Kennou, S. *Org. Electrochem.* **2009**, *10*, 1382–1387. (b) Petraki, F.; Kennou, S.; Nespurek, S. *J. Appl. Phys.* **2008**, *103*, 033710–1−6.
(6) Latteyer, F.; Peisert, H.; Aygül, U.; Biswas, I.; Petraki, F.; Basova, T.; Vollmer, A.; Chassé, T. *J. Phys. Chem. C* **2011**, *115*, 11657–11665.
(7) Hein, C.; Mankel, E.; Mayer, T.; Jaegermann, W. *Sol. Energy Mater. Sol. Cells* **2010**, *94*, 662–667.
(8) Liao, M. S.; Scheiner, S. *J. Comput. Chem.* **2002**, *223*, 1391–1403.
(9) Molodtsova, O. V.; Knupfer, M.; Ossipyan, Yu. A.; Aristov, V. Yu. *J. Appl. Phys.* **2008**, *104*, 083704−1–5.
(10) Kirner, J. F.; Dow, W.; Scheidt, W. R. *Inorg. Chem.* **1976**, *15*, 1685–1690.
(11) Zhao, A.; Li, Q.; Chen, L.; Xiang, H.; Wang, W.; Pan, S.; Wang, B.; Xiao, X.; Yang, J.; Hou, J. G. *Science* **2005**, *309*, 1542–1544.
(12) Kroll, T.; Aristov, V. Yu.; Molodtsova, O. V.; Ossipyan, Yu. A.; Vyalikh, D. V.; Buechner, B.; Knupfer, M. *J. Phys. Chem. A* **2009**, *113*, 8917–8922.
(13) Bogani, L.; Wernsdorfer, W. *Nat. Mater.* **2008**, *7*, 179–186.
(14) Heutz, S.; Mitra, C.; Wu, W.; Fisher, A. J.; Kerridge, A.; Stoneham, M.; Harker, T. H.; Gardener, J.; Tseng, H. -H.; Jones, T. S.; Renner, C.; Aeppli, G. *Adv. Mater.* **2007**, *19*, 3618–3622.
(15) Javaid, S.; Bowen, M.; Boukari, S.; Joly, L.; Beaufrand, J. -B.; Chen, Xi; Dappe, Y. J.; Scheurer, F.; Kappler, J. -P.; Arabski, J.; Wulfhekel, W.; Alouani, M.; Beaurepaire, E. *Phys. Rev. Lett.* **2010**, *105*, 077201−1–4.
(16) Atodiresei, N.; Brede, J.; Lazić, P.; Caciuc, V.; Hoffmann, G.; Wiesendanger, R.; Blügel, S. *Phys. Rev. Lett.* **2010**, *105*, 066601−1−4.
(17) (a) Schaffer, A. M.; Gouterman, M.; Davidson, E. R. *Theor. Chim. Acta* **1973**, *30*, 9–30. (b) Mathur, S. C.; Singh, J. *Int. J. Quantum Chem.* **1972**, *VI*, 57–82.
(18) Petraki, F.; Peisert, H.; Biswas, I.; Chassé, T. *J. Phys. Chem. C* **2010**, *114*, 17638–17643.
(19) Grobosch, M.; Mahns, B.; Loose, C.; Friedrich, R.; Schmidt, C.; Kortus, J.; Knupfer, M. *Chem. Phys. Lett.* **2011**, *505*, 122–125.
(20) Li., Z.; Li, B.; Yang, J.; Hou, J. G. *Acc. Chem. Res.* **2010**, *43*, 954–962.
(21) Stradi, D.; Díaz, C.; Martín, F.; Alcamí, M. *Theor. Chem. Acc.* **2011**, *128*, 497–503.
(22) Shang, M -H; Nagaosa, M.; Nagamatsu, S.; Hosoumi, S.; Kera, S.; Fujikawa, T.; Ueno, N. *J. Electron Spectrosc. Relat. Phenom.* **2010**, *184*, 261–264.
(23) Vilmercati, P.; Cvetko, D.; Cossaro, A.; Morgante, A. *Surf. Sci.* **2009**, *603*, 1542–1556.
(24) Haeming, M.; Weinhardt, L.; Schoell, A.; Reinert, F. *Chem. Phys. Lett.* **2011**, *510*, 82–86.
(25) Petraki, F.; Peisert, H.; Biswas, I.; Aygül, U.; Latteyer, F.; Vollmer, A.; Chassé, T. *J. Phys. Chem. Lett.* **2010**, *1*, 3380–3384.
(26) Stöhr, J.; Outka, D. A. *Phys. Rev. B* **1987**, *36*, 7891–7905.
(27) Alfredsson, Y.; Åhlund, J.; Nilson, K.; Kjeldgaard, L.; O'Shea, J. N.; Theobald, J.; Bao, Z.; Mårtensson, N.; Sandell, A.; Puglia, C.; Siegbahn, H. *Thin Solid Films* **2005**, *493*, 13–19.

(28) (a) Peisert, H.; Biswas, I.; Knupfer, M.; Chassé, T. *Phys. Status Solidi B* **2009**, *246*, 1529–1545. (b) Biswas, I.; Peisert, H.; Casu, M. B.; Schuster, B. -E.; Merz, M.; Schuppler, S.; Chassé, T.; Nagel, P. *Phys. Status Solidi A* **2009**, *206*, 2524–2528.
(29) Takada, M.; Tada, H. *Chem. Phys. Lett.* **2004**, *392*, 265–269.
(30) Koch, E. E.; Jugnet, Y.; Himpsel, F. J. *Chem. Phys. Lett.* **1985**, *116*, 7–11.
(31) Rocco, M. L. M.; Frank, K. -H.; Yannoulis, P.; Koch, E. -E. *J. Chem. Phys.* **1990**, *93*, 6859–6864.
(32) Floreano, L.; Cossaro, A.; Gotter, R.; Verdini, A.; Bavdek, G.; Evangelista, F.; Ruocco, A.; Morgante, A.; Cvetko, D. *J. Phys. Chem. C* **2008**, *112*, 10794–10802.
(33) Liao, M. S.; Scheiner, S. *J. Chem. Phys.* **2001**, *114*, 9780–9791.
(34) Peisert, H.; Biswas, I.; Aygül, U.; Vollmer, A.; Chassé, T. *Chem. Phys. Lett.* **2010**, *493*, 126–129.
(35) Aristov, V. Yu.; Molodtsova, O. V.; Knupfer, M. *Org. Electrochem.* **2011**, *12*, 372–375.
(36) Toader, M.; Knupfer, M.; Zahn, D. R. T.; Hietschold, M. *Surf. Sci.* **2011**, *605*, 1510–1515.
(37) Gargiani, P.; Angelucci, M.; Mariani, C.; Betti, M. G. *Phys. Rev. B* **2010**, *81*, 085412–1−7.
(38) Betti, M. G.; Gargiani, P.; Frisenda, R.; Biagi, R.; Cossaro, A.; Verdini, A.; Floreano, L.; Mariani, C. *J. Phys. Chem. C* **2010**, *114*, 21638–21644.
(39) Baran, J. D.; Larsson, J. A.; Woolley, R. A. J.; Cong, Y.; Moriarty, P. J.; Cafolla, A. A.; Schulte, K.; Dhanak, V. R. *Phys. Rev. B* **2010**, *81*, 075413–1−12.
(40) Buchner, F.; Warnick, K. -G.; Woelfle, T.; Goerling, A.; Steinrueck, H. -P.; Hieringer, W.; Marbach, H. *J. Phys. Chem. C* **2009**, *113*, 16450–16457.
(41) Bai, Y.; Sekita, M.; Schmid, M.; Bischof, T.; Steinrueck, H. -P.; Gottfried, J. M. *Phys. Chem. Chem. Phys.* **2010**, *12*, 4336–4344.
(42) Toader, M.; Gopakumar, T. G.; Shukrynau, P.; Hietschold, M. *J. Phys. Chem. C* **2010**, *114*, 21548–21554.
(43) Zhao, A.; Hu, Z.; Wang, B.; Xiao, X.; Yang, J.; Hou, J. G. *J. Chem. Phys.* **2008**, *128*, 234705−1–6.
(44) Kawai, J.; Mizutani, Y.; Sugimura, T.; Sai, M.; Higuchi, T.; Harada, Y.; Ishiwata, Y.; Fukushima, A.; Fujisawa, M.; Watanabe, M.; Maeda, K.; Shin, S.; Gohshi, Y. *Spectrochim. Acta, Part B* **2000**, *55*, 1385–1395.
(45) Nelson, A. J.; Reynolds, J. G.; Roos, J. W. *J. Vac. Sci. Technol., A* **2000**, *18*, 1072–1076.
(46) Grobosch, M.; Schmidt, C.; Kraus, R.; Knupfer, M. *Org. Electrochem.* **2010**, *11*, 1483–1488.
(47) de Groot, F. M. F. *Coord. Chem. Rev.* **2005**, *249*, 31–63.
(48) Li, F.; Zhenga, Q.; Yanga, G.; Lu, L. *Dyes Pigm.* **2008**, *77*, 277–280.
(49) Shen, X.; Sun, L.; Yi, Z.; Benassi, E.; Zhang, R.; Shen, Z.; Sanvito, S.; Hou, S. *Phys. Chem. Chem. Phys.* **2010**, *12*, 10805–10811.
(50) Marom, N.; Kronik, L. *Appl. Phys. A: Mater. Sci. Process.* **2009**, *95*, 165–172.